Hydrol. Earth Syst. Sci. Discuss., 11, 11183–11202, 2014
www.hydrol-earth-syst-sci-discuss.net/11/11183/2014/
doi:10.5194/hessd-11-11183-2014

Hydrology and Earth System Sciences
Discussions
Open Access

Do changes in climate or vegetation regulate evapotranspiration and streamflow trends in water-limited basins?

Q. Liu[1,2], Z. Yang[1,2], L. Liang[3], and W. Nan[1,2]

[1]Key Laboratory for Water and Sediment Sciences, Ministry of Education, School of Environment, Beijing Normal University, Beijing 100875, China
[2]State Key Laboratory of Water Environment Simulation, School of Environment, Beijing Normal University, Beijing 100875, China
[3]Key Laboratory of Tibetan Environment Changes and Land Surface Processes, Institute of Tibetan Plateau Research, Chinese Academy of Sciences, Beijing 100101, China

Received: 9 July 2014 – Accepted: 2 September 2014 – Published: 9 October 2014

Correspondence to: Q. Liu (liuqiang@bnu.edu.cn)

Published by Copernicus Publications on behalf of the European Geosciences Union.

Abstract

Interactions between climate change, vegetation, and soil regulate hydrological processes. In this study, it was assumed that vegetation type and extent remained fixed and unchanged throughout the study period, while the effective rooting depth (Z_e) changed under climate change scenarios. Budyko's hydrological model was used to explore the impact of climate change and vegetation on evapotranspiration (E) and streamflow (Q) on the static vegetation rooting depth and the dynamic vegetation rooting depth. Results showed that both precipitation (P) and potential evapotranspiration (E_p) exhibited negative trends, which resulted in decreasing trends for dynamic Z_e scenarios. Combined with climatic change, decreasing trends in Z_e altered the partitioning of P into E and Q. For dynamic scenarios, total E and Q were predicted to be −1.73 and 28.22 %, respectively, greater than static scenarios. Although climate change regulated changes in E and Q, the response of Z_e to climate change had a greater overall contribution to changes in hydrological processes. Results from this study suggest that with the exception of vegetation type and extent, Z_e scenarios were able to alter water balances, which in itself should help to regulate climate change impacts on water resources.

1 Introduction

Partitioning of precipitation (P) on land surfaces into evapotranspiraiton (E) and streamflow (Q) reflects a hydrologic response to land use and climate forcing. Given that this impacts water availability globally (Xu et al., 2013), understanding such a process is critical for water resource management. In the past, a large number of studies have been conducted to quantify the impact of climate or vegetation changes on catchment water balances. Evidence shows that changes in climatic conditions, resulting from P and potential evapotranspiration E_p, for example, have a considerable impact on Q (e.g., IPCC, 2007; Oudin et al., 2009; Liang et al., 2013). Additionally, changes in

HESSD
11, 11183–11202, 2014

land use type can dramatically alter water balances on different scales, such as the reduction in Q observed on the Loess Plateau, China, which the Grain for Green program has shown to exist. Thus, quantifying the impact of climate and vegetation change on Q remains a challenge in hydrological sciences.

Along with complex, physically based distributed hydrological models (bottom-up approach), a simple coupled water and energy balance model (top-down approach), such as Budyko's hydrological model, has attracted considerable attention in recent years (e.g., Zhang et al., 2001; Yang et al., 2007; Brümmer et al., 2012; Donohue et al., 2012). According to Budyko's assumption (1974), available water and energy are the primary factors that determine the rate of E, which also controls the partitioning of P into E and Q. Because the original version of Budyko's assumption only included climatic variables, an adjustable parameter has been incorporated into the model to reflect the influence of watershed characteristics (e.g., Fu et al., 1981; Choudhury, 1999; Zhang et al., 2001; Yang et al., 2007). Even though this watershed characteristics parameter (n) has been investigated by a number of studies (Zhang et al., 2001; Yang et al., 2009; Donohue et al., 2010), its relation to physical attributes remains obscure (Gerrits et al., 2009; Donohue et al., 2012; Liu and McVicar, 2012). By combining equations by Choudhury (1999) and Porporato et al. (2004), Donohue et al. (2012) deduced the relationship between n and ecohydrological processes (such as storm depth α, plant-available soil water holding capacity κ, and the effective rooting depth Z_e), which offers new insight into understanding the response of hydrological processes to impacts of climate change and vegetation. While numerous studies have investigated impacts of climate and vegetation on hydrological processes in the past, few have explored impacts of vegetation on hydrological processes from the point of view of the response of vegetation to climate change. The objective of this study was therefore to explore the temporal trends in E and Q, and to assess the relative contribution of climate and vegetation change to E and Q.

HESSD
11, 11183–11202, 2014

2 Hydrological model and data set

This study employed the improved version of Budyko's hydrological model with the addition of an ecohydrological adjustable parameter to assess impacts of climate and vegetation changes on E and Q. By incorporating this adjustment parameter, Budyko's model can be expressed as follows (e.g., Choudhury's equation (1999)):

$$E = \frac{PE_\mathrm{p}}{\left(P^n + E_\mathrm{p}^n\right)^{(1/n)}}, \tag{1}$$

where n is a catchment-specific parameter (dimensionless), which reflects the influence of catchment characteristics on the partitioning of P between E and Q. By combining the equation provided by Porporato et al. (2004) and Choudhury (1999), Donohue et al. (2012) used the effective rooting depth (Z_e), the mean depth per storm event (α), and the fractional plant-available water holding capacity (κ) to explain n.

$$n = 0.21\frac{\kappa Z_\mathrm{e}}{\alpha} + 0.60. \tag{2}$$

Ignoring changes in storage, the steady state water balance model can be expressed as follows (Donohue et al., 2011; Roderick and Farquhar, 2011; Liu and McVicar, 2012):

$$Q = P - E = P - \frac{PE_\mathrm{p}}{\left(P^n + E_\mathrm{p}^n\right)^{(1/n)}}. \tag{3}$$

Equations (2) and (3) constitute the Budyko–Choudhury–Porporato model (BCP model). By incorporating ecohydrological parameters (Z_e, α, and κ), this model can be used to assess the impact of climate change on E or Q.

The Yellow River basin (YRB) is approximately 5400 km long, with a basin drainage area of 7.95×10^5 km^2. Its headwaters originate from the Tibetan Plateau, flowing

HESSD
11, 11183–11202, 2014

Title Page
Abstract Introduction
Conclusions References
Tables Figures
◀| |▶
◀ ▶
Back Close
Full Screen / Esc
Printer-friendly Version
Interactive Discussion

through the Loess Plateau and the North China Plain before finally emptying into the Bohai Sea. Impacted by climate change, most YRB regions have exhibited decreasing P trends (Liu et al., 2008; McVicar et al., 2002; Nakayama, 2011). Along with climate change, alterations in physiological characteristics (e.g., changes in Z_e) can also have an impact on changes in hydrological processes, although little effort has been focused on this topic to date. In this study, it was assumed that vegetation type and extent were fixed and remained unchanged throughout the study period, while the effective rooting depth changed under the influence of climatic change. Two scenarios were developed for this study according to Budyko's assumption. For the static Z_e scenario, the effective rooting depth for 1961 was fixed throughout a simulation period between 1961 and 2010. For the dynamic Z_e scenario, the effective rooting depth was influenced by the specific water and energy conditions of each grid cell, in accordance with specific changes in climatic conditions. Data from the National Climate Center of the China Meteorological Administration (CMA) were used to investigate impacts of climate change on water resources. The Yellow River Conservancy Commission (YRCC) provided Q data between 1961 and 2010. Monthly E_p was calculated by means of monthly wind speed, daylight hours, relative humidity, and average air temperature using the Penman equation (Shuttleworth, 1993). Normalized difference vegetation index (NDVI) data were obtained from the Global Land Cover Facility (http://www.glcf.umd.edu/), and were used to calculate the fraction of photosynthetically active radiation (PAR) absorbed by vegetation (f_{PAR}).

3 Results

3.1 Changes to ecohydrological processes

YRB P and E_p temporal trends (1961–2010) are provided in Fig. 1. On a basin scale, the average slope for P was $-0.96\,mm\,a^{-2}$, with a range from $-2.37\,mm\,a^{-2}$ to $1.03\,mm\,a^{-2}$ (Fig. 1a), while the average slope for E_p was $-0.13\,mm\,a^{-2}$, with a range

HESSD
11, 11183–11202, 2014

from −3.38 to 1.47 mm a^{-2} (Fig. 1b). E_p and P exhibited increasing trends, with an average increase of 0.004 mm a^{-2}. The vegetation fractions for trees (Fig. 1c) and grass (Fig. 1d) were calculated from f_{PAR} (Donohue et al., 2009), which was necessary for calculating Z_e.

According to conclusions that state that the higher the P the deeper the Z_e (Schenk and Jackson, 2002; Donohue et al., 2012), Z_e was calculated for YRB, a large water-limited basin (data provided in Fig. 2). Averaged static Z_e (Fig. 2a) (1961 was used to set the base condition of Z_e) ranged from 89 to 2245 mm, with an average of 381 mm, while averaged Z_e throughout 1961–2010 ranged from 82 to 1818 mm. Z_e was influenced by decreasing P trends, resulting in a decreasing trend with a slope of −0.12 mm a^{-2}.

3.2 Changes in streamflow and evapotranspiration

Modeled time series of E are provided in Fig. 3. Results showed similar trends to observed E (calculated using $P-Q$). Furthermore, the Nash–Sutcliffe model efficiency (NSE) coefficient reached up to 0.85 for the dynamic Z_e scenario. As a result of the overestimation of high E (i.e., 1961 and 1964) and the underestimation of high E (i.e., 2002), modeled E under the dynamic Z_e scenario exhibited a negative trend (−0.81 mm a^{-2}), and thus was in opposition to observations (0.23 mm a^{-2}). Modeled E under the static Z_e scenario also exhibited a negative trend, with a slope of −0.78 mm a^{-2}.

Relative differences in modeled annual total Q and E between the static Z_e and dynamic Z_e scenarios are provided in Fig. 4. Results showed that (i) for the dynamic Z_e scenario (Fig. 4a), total E was predicted to be 1.73 % smaller than the static Z_e scenario, while, conversely, total Q (Fig. 4b) was predicted to be 28.22 % greater than the static Z_e scenario, and (ii) decreasing trends were detected in most areas of the basin for E, while increasing trends were detected in most areas of the basin for Q.

3.3 Relative contribution of climatic and vegetation change on E and Q

Temporal trends in E calculated from both dynamic and static Z_e scenarios are respectively provided in Fig. 5a and b. Results showed that (i) temporal trends for both dynamic and static Z_e scenarios exhibited similar spatial patterns; i.e., most areas of the basin contributed to negative (decreasing) trends, and only the northwestern area contributed to positive (increasing) trends in E, (ii) temporal trends in E under the dynamic Z_e scenario ranged from -2.86 to $1.41\,\mathrm{mm\,a^{-2}}$, with an average increase of $-0.80\,\mathrm{mm\,a^{-2}}$ (Fig. 5a), while temporal trends in E under the static Z_e scenario ranged from -2.70 to $1.41\,\mathrm{mm\,a^{-2}}$, with an average increase of $-0.81\,\mathrm{mm\,a^{-2}}$ (Fig. 5b), and (iii) significant trends ($P < 0.05$) in E under dynamic (Fig. 5c) and static Z_e scenarios (Fig. 5d) showed similar patterns for YRB, while the extent per area showed significant increasing trends under the static Z_e scenario (Fig. 5d).

The relative contribution of climate was mapped as the trend of modeled E under the dynamic Z_e scenario divided by modeled E under the static Z_e scenario for each grid cell (Fig. 6a) from which the relative contribution of vegetation was obtained (Fig. 6b). Results showed that climate regulated temporal trends in E, while changes in Z_e only contributed slightly to changes in E. Using the differential of E or Q to the variables (e.g., $\partial E/\partial P$) multiplied by changes in variables (e.g., dP), the contribution of different variables can be obtained ($\partial E/\partial P \times \mathrm{d}P$). For example, following Donohue et al. (2012), the "typical variability" observed for each variable between 1961 and 2010 was determined (represented by the standard deviation of annual values). Results showed that (i) changes in P caused the greatest variability in E (or Q), generally followed by variability in Z_e, α, and E_p, (ii) changes in P contributed more to changes in E compared to Q, and (iii) summed contributions of climatic variables (P, E_p, and α) to E and Q were larger than Z_e, especially for E.

4 Discussion

As demonstrated by results from this study (Fig. 1), both P and E_p showed decreasing trends, while E_p/P showed a slight increasing trend (0.004 mm a^{-2}) throughout the 1961–2010 period. Results were consistent with those reported by Liu and McVicar (2012). Decreasing trends in P (with an average increase of −0.96 mm a^{-2}) or increasing trends in E_p/P resulted in decreasing trends in Z_e (data provided in Fig. 2). Strong interactions are known to exist between climate, vegetation, and soil properties that lead to specific hydrologic partitioning on a catchment scale (Troch et al., 2013). Inevitably, it is the available water (P) and energy (represented by E_p) that regulate vegetation patterns. Degradation in vegetation influenced by decreasing P has been reported in YRB (e.g., Xin et al., 2008). In particular, changes in vegetation extent and type (mainly resulting from human activity) are major causes of Q change (Li et al., 2007; Liu et al., 2009). For example, changes in vegetation patterns as a result of land use changes (e.g., such as determined by the Grain for Green program in the Loess Plateau) inevitably alter hydrological processes, and result in a decrease in Q (McVicar et al., 2007; Cao et al., 2011). On the one hand, numerous studies concluded that vegetation change was the main cause of hydrological process change, e.g., such as observed changes in Q in the Yiluo River basin (Liu et al., 2009). On the other hand, other studies reported that climate variability in certain regions influences surface hydrology more significantly compared to land use changes, e.g., such as observed in the Heihe River basin, China (Li et al., 2009), as well as the upper Mississippi River basin (Frans et al., 2013).

In combination with climate change, this study explored how vegetation impacts hydrological processes from an alternative aspect, i.e., assessing Z_e response to climate change and its impacts on Q and E. According to Budyko's assumption, the greater the P, the deeper the rooting depth (Schenk and Jackson, 2002). Furthermore, modeled E under dynamic and static Z_e scenarios exhibited negative trends, while observed E exhibited positive trends (Fig. 3). Vegetation structure profoundly regulates the annual

HESSD
11, 11183–11202, 2014

surface hydrological cycle, and is a cause and consequence of surface water balances (Gentine et al., 2012). In this study, following Donohue et al. (2012), Z_e in combination with α and κ was used to calculated n (1.81 average). Results were similar to n ($n = 1.76$) calculated from a nonlinear fitted model by Liu and McVicar (2012). Given that Z_e data are scarce, validation of modeled Z_e is difficult to obtain for larger basins (Donohue et al., 2012). From the n calculated for each grid cell, it was shown that simulated E and Q fitted well with observed values (provided in Fig. 3). Alteration of Z_e contributed more to changes in Q and E (Fig. 4 and Table 1), which indicated that the response of vegetation to climatic change can alter the partitioning of P into E and Q. Budyko's hydrological model with the addition of ecohydrological parameters (such as Z_e, α, and κ) captured affects of watershed characteristics on the partitioning of P into E and Q. Results can also reflect relative contributions provided in Fig. 5 and Fig. 6. For example, Fig. 5c and d show that significant temporal trends in E yield different results between dynamic and static Z_e scenarios. Figure 6 shows that climate change regulates temporal trend changes in E, which are consistent with results provided in Table 1. Furthermore, given that soil, topography, vegetation, and climate are intrinsically interconnected, Gentine et al. (2012) attempted to use the Budyko curve to explain ecohydrological controls of soil water balances. Further research should focus more attention on mechanisms of watershed parameters and improve the accuracy of the Budyko's hydrological model, as it relates to different temporal and spatial scales.

5 Conclusions

Climate change and vegetation impacts on Q and E can be explored using Budyko's hydrological model with the addition of adjustable ecohydrological parameters (such as Z_e, α, and κ). According to the "typical variability" of different variables, climate change and vegetation impacts were obtained for the dynamic and static Z_e scenarios investigated. The following conclusions can be drawn from this study:

1. For YRB, both P and E_p exhibited negative trends, while E_p/P exhibited positive trends, resulting in a decreasing Z_e trend under the dynamic Z_e scenario throughout the 1961–2010 investigation.

2. Simulated E under the dynamic and static Z_e scenarios exhibited negative trends, with an average increase of −0.81 and −0.78 $mm\,a^{-2}$, respectively. For the dynamic scenario, total E and Q were respectively predicted to be −1.73 and 28.22 % greater than the static scenario, which exhibited obvious spatial variation.

3. As anticipated, although climate change regulates changes in E and Q, Z_e response to climate change contributed more to changes in hydrological processes for this water-limited region. Results indicated that with the exception of vegetation type and extent, Z_e scenarios were able to alter the partitioning of P into E and Q.

Acknowledgements. This study was supported by the Major State Basic Research Development Program of China (973 Program) (no. 2010CB951104), the National Science Foundation for Innovative Research Group (no. 51121003), the Fundamental Research Funds for the Central Universities (no. 2012LYB12), and the Beijing Higher Education Young Elite Teacher Project (no. YETP0259). We would like to thank the National Meteorological Information Center, the China Meteorological Administration, and the Yellow River Conservancy Commission for providing meteorological and streamflow data.

References

Allen, R. G., Pereira, L. S., Raes, D., and Smith, M.: Crop evapotranspiration: guidelines for computing crop water requirement, FAO Irrig., and Drain. Paper No. 56, FAO, Rome, Italy, 1988.

Bonan, G. B.: Observational evidence for reduction of daily maximum temperature by croplands in the Midwest United States, J. Climate, 14, 2430–2442, 2001.

Brümmer, C., Black, T. A., Jassal, R. S., Grant, N. J., Spittlehouse, D. L., Chen, B., Nesic, Z., Amiro, B. D., Arain, M. A., Barr, A. G., Bourque, C. P. A., Coursolle, C., Dunn, A. L., Flanagan, L. B., Humphreys, E. R., Lafleur, P. M., Margolis, H. A., McCaughey, J. H., and Wofsy, S. C.: How climate and vegetation type influence evapotranspiration and water use efficiency in Canadian forest, peatland and grassland ecosystems, Agr. Forest Meteorol., 153, 14–30, 2012.

Budyko, M. I.: Climate and Life, Academic Press, INC. (London) LTD, 508 pp., 1974.

Cao, S. X., Chen, L., Shankman, D., Wang, C., Wang, X., and Zhang, H.: Excessive reliance on afforestation in China's arid and semi-arid regions: lessons in ecological restoration, Earth-Sci. Rev., 104, 240–245, 2011.

Choudhury, B. J.: Evaluation of an empirical equation for annual evaporation using field observations and results from a biophysical model, J. Hydrol., 216, 99–110, 1999.

Donohue, R. J., Roderick, M. L., and McVicar, T. R.: Can dynamic vegetation information improve the accuracy of Budyko's hydrological model?, J. Hydrol., 390, 23–34, 2010.

Donohue, R. J., Roderick, M. L., and McVicar, T. R.: Assessing the differences in sensitivities of runoff to changes in climatic conditions across a large basin, J. Hydrol., 406, 234–244, 2011.

Donohue, R. J., Roderick, M. L., and McVicar, T. R.: Roots, storms and soil pores: incorporating key ecohydrological processes into Budyko's hydrological model, J. Hydrol., 436–437, 35–50, 2012.

Frans, C., Istanbulluoglu, E., Mishra, V., Munoz-Arriola, F., and Lettenmaier, D. P.: Are climatic or land cover changes the dominant cause of runoff trends in the Upper Mississippi River Basin?, Geophys. Res. Lett., 40, 1104–1110, doi:10.1002/grl.50262, 2013.

Fu, B. P.: On the calculation of the evaporation from land surface, Scientia. Atmosp. Sinica, 5, 23–31, 1981 (in Chinese).

Gentine, P., D'Odorico, P., Lintner, B. R., Sivandran, G., and Salvucci, G.: Interdependence of climate, soil, and vegetation as constrained by the Budyko curve, Geophys. Res. Lett., 39, L19404, doi:10.1029/2012GL053492, 2012.

Gerrits, A. M. J., Savenije, H. H. G., Veling, E. J. M., and Fister, L. P.: Analytical derivation of the Budyko curve based on rainfall characteristics and a simple evaporation model, Water Resour. Res., 45, W04403, doi:10.1029/2008WR007308, 2009.

IPCC: Climate Change 2007: The Physical Science Basis. Contribution of Working Group I to the Fourth Assessment, Camb. U. Pr., New York, 2007.

Li, L. J., Zhang, L., Wang, H., Wang, J., Yang, J. W., Jiang, D. J., Li, J. Y., and Qin, D. Y.: Assessing the impact of climate variability and human activities on streamflow from the Wuding River basin in China, Hydrol. Process., 21, 3485–3491, 2007.

Li, Z., Liu, W. Z., Zhang, X. C., and Zheng, F. L.: Impacts of land use change and climate variability on hydrology in an agricultural catchment on the Loess Plateau of China, J. Hydrol., 377, 35–42, 2009.

Liang, L. Q. and Liu, Q.: Streamflow sensitivity analysis to climate change for a large water-limited basin, Hydrol. Process., doi:10.1002/hyp.9720, 2013.

Liu, Q. and McVicar, T. M.: Assessing climate change induced modification of Penman potential evaporation and runoff sensitivity in a large water-limited basin, J. Hydrol., 464–465, 352–262, 2012.

Liu, Q. and Yang, Z. F.: Quantitative estimation of the impact of climate change on actual evapotranspiration in the Yellow River Basin, China, J. Hydrol., 395, 226–234, 2010.

Liu, Q., Yang, Z. F., and Cui, B. S.: Spatial and temporal variability of annual precipitation during 1961–2006 in Yellow River Basin, China, J. Hydrol., 361, 330–338, 2008.

Liu, Q., Yang, Z. F., Cui, B. S., and Sun, T.: Temporal trends of Hydro-climatic variables and runoff response to climatic variability and vegetation changes in the Yiluo River basin, China, Hydrol. Process., 23, 3030–3039, 2009.

McVicar, T. R., Zhang, G. L., Bradford, A. S., Wang, H. X., Dawes, W. R., Zhang, L., and Li, L. T.: Monitoring regional agricultural water use efficiency for Hebei Province on the North China Plain, Aust. J. Agr. Res., 53, 55–76, 2002.

McVicar, T. R., Li, L. T., Van Niel, T. G., Zhang, L., Li, R., Yang, Q. K., Zhang, X. P., Mu, X. M., Wen, Z. M., Liu, W. Z., Zhao, Y. A., Liu, Z. H., and Gao, P.: Developing a decision support tool for China's re-vegetation program: simulating regional impacts of afforestation on average annual streamflow in the Loess Plateau, Forest Ecol. Manag., 251, 65–81, 2007.

Nakayama, T.: Simulation of the effect of irrigation on the hydrologic cycle in the highly cultivated Yellow River Basin, Agr. Forest Meteorol., 151, 314–327, 2011.

Oudin, L., Andreassian, V., Lerat, J., and Michel, C.: Has land cover a significant impact on mean annual streamflow? An international assessment using 1508 catchments, Hydrol. J., 357, 303–316, 2008.

Porporato, A., Daly, E., and Rodriguez-Iturbe, I.: Soil water balance and ecosystem response to climate change, Am. Nat., 164, 625–632, 2004.

Roderick, M. L. and Farquhar, G. D.: A simple framework for relating variations in runoff to variations in climatic conditions and catchment properties, Water Resour. Res., 47, W00G07, doi:10.1029/2010WR009826, 2011.
Schenk, H. J. and Jackson, R. B.: Rooting depths, lateral root spreads and below-ground/above-ground allometries of plants in water-lmited ecosystems, J. Ecol., 90, 480–494, 2002.
Shuttleworth, W. J.: Evaporation, in: Handbook Hydrol., edited by: Maidment, D. R., McGraw-Hill, Sydney, 1993.
Troch, P. A., Carrillo, G., Sivapalan, M., Wagener, T., and Sawicz, K.: Climate-vegetation-soil interactions and long-term hydrologic partitioning: signatures of catchment co-evolution, Hydrol. Earth Syst. Sci., 17, 2209–2217, doi:10.5194/hess-17-2209-2013, 2013.
Xin, Z. B., Xu, J. X., and Wei, Z.: Spatiotemporal variations of vegetation cover on the Chinese Loess Plateau (1981–2006): impacts of climate changes and human activities, Sci. China Ser. D, 51, 67–78, 2008.
Xu, X. L., Liu, W., Scanlon, B. R., Zhang, L., and Pan, M.: Local and global factors controlling water-energy balances within the Budyko framework, Geophys. Res. Lett., 40, 6123–6129, 2013.
Yang, D. W., Sun, F. B., Liu, Z. Y., Cong, Z. T., Ni, G. H., and Lei, Z. D.: Analyzing spatial and temporal variability of annual water-energy balance in non-humid regions of China using the Budyko hypothesis, Water Resour. Res., 43, W04426, doi:10.1029/2006WR005224, 2007.
Yang, D. W., Shao, W. W., Yeh, P. J. F., Yang, H. B., Kanae, S., and Oki, T.: Impact of vegetation coverage on regional water balance in the non-humid regions of China, Water Resour. Res., 45, W00A14, doi:10.1029/2008WR006948, 2009.
Yang, H., Yang, D., Lei, Z., and Sun, F.: New analytical derivation of the mean annual water balance equation, Water Resour. Res., 44, W03410, doi:10.1029/2007WR006135, 2008.
Zhang, L., Dawes, W. R., and Walker, G. R.: The response of mean annual evapotranspiration to vegetation changes at catchment scale, Water Resour. Res., 37, 701–708, 2001.

HESSD
11, 11183–11202, 2014

Changes in climate or vegetation

Q. Liu et al.

HESSD
11, 11183–11202, 2014

Changes in climate or vegetation

Q. Liu et al.

Table 1. Summaries of E and Q sensitivities to changes in ecohydrological conditions throughout the study period (1961–2010). Shown for each variable and zone are E and Q sensitivity coefficients, observed variability per variable, and typical variability in E caused by driving variables. dZ_e is the difference between tree and grass Z_e modeled for the basin.

	Unit	YRB		Unit	YRB
$\partial E/\partial P$	$mm\,a^{-1}/mm\,a^{-1}$	0.73	$\partial Q/\partial P$	$mm\,a^{-1}/mm\,a^{-1}$	0.17
dP	$mm\,a^{-1}$	59	dP	$mm\,a^{-1}$	59
$\partial E/\partial P \times dP$	$mm\,a^{-1}$	41.9	$Q/\partial P \times dP$	$mm\,a^{-1}$	10.1
$\partial E/\partial E_p$	$mm\,a^{-1}/mm\,a^{-1}$	0.05	$\partial Q/\partial E_p$	$mm\,a^{-1}/mm\,a^{-1}$	−0.05
dE_p	$mm\,a^{-1}$	42	dE_p	$mm\,a^{-1}$	42
$\partial E/\partial_{Ep} dE_p$	$mm\,a^{-1}$	2.1	$\partial Q/\partial_{Ep} \times dE_p$	$mm\,a^{-1}$	−2.1
$\partial E/\partial \alpha$	$mm\,a^{-1}/mm$	−10.6	$\partial Q/\partial \alpha$	$mm\,a^{-1}/mm$	10.6
$d\alpha$	mm	0.39	$d\alpha$	mm	0.39
$\partial E/\partial \alpha \times d\alpha$	$mm\,a^{-1}$	−4.2	$\partial Q/\partial \alpha \times d\alpha$	$mm\,a^{-1}$	4.2
$\partial E/\partial Z_e$	$mm\,a^{-1}/mm$	0.17	$\partial Q/\partial Z_e$	$mm\,a^{-1}/mm$	−0.17
dZ_e	mm	30	dZ_e	mm	30
$\partial E/\partial Z_e \times dZ_e$	$mm\,a^{-1}$	5	$\partial E/\partial Z_e \times dZ_e$	$mm\,a^{-1}$	−5

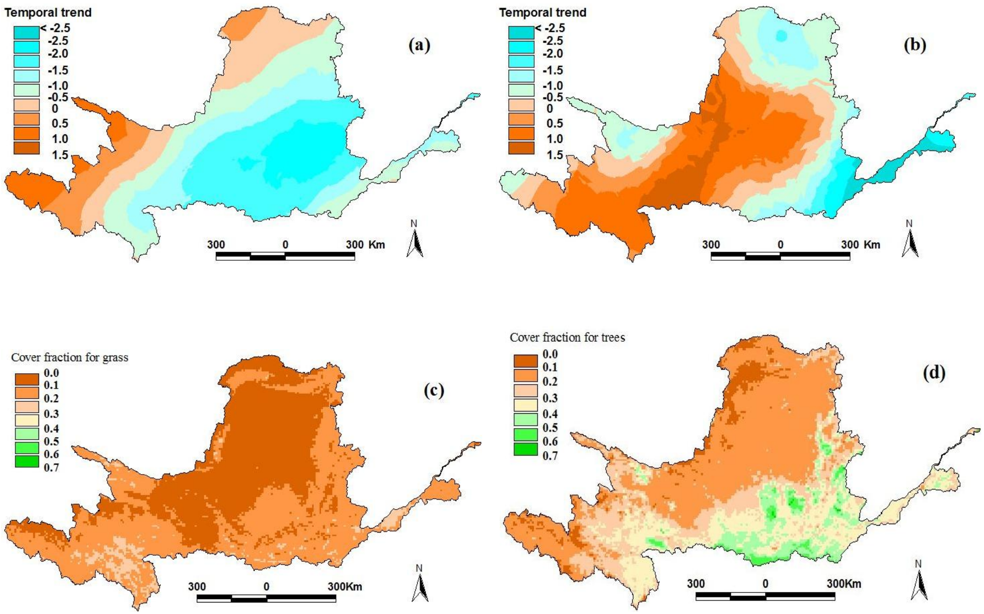

Figure 1. Temporal trends in P **(a)** and E_p **(b)** (mm a^{-2}), and the cover fraction for grass **(c)** and trees **(d)**.

Discussion Paper | Discussion Paper | Discussion Paper | Discussion Paper |

HESSD
11, 11183–11202, 2014

Changes in climate or vegetation

Q. Liu et al.

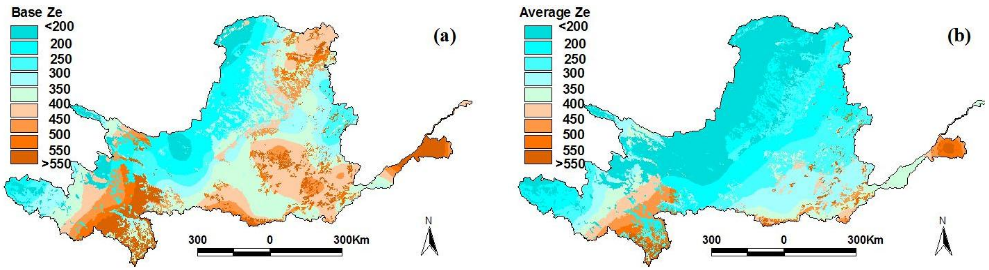

Figure 2. Static Z_e (1961) **(a)** and average dynamic Z_e **(b)** (1961–2010) for the Yellow River basin, China.

HESSD
11, 11183–11202, 2014
Changes in climate or vegetation
Q. Liu et al.

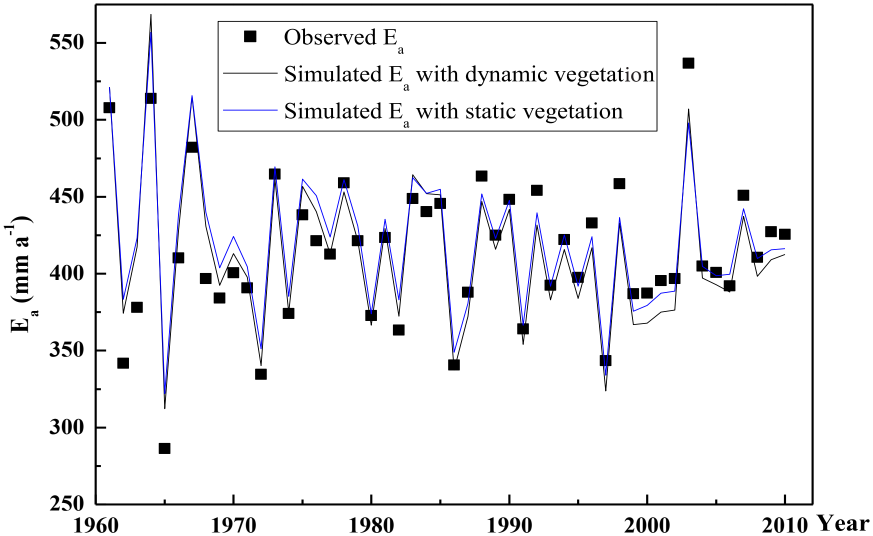

Figure 3. Observed and modeled annual *E* for the Yellow River basin, China.

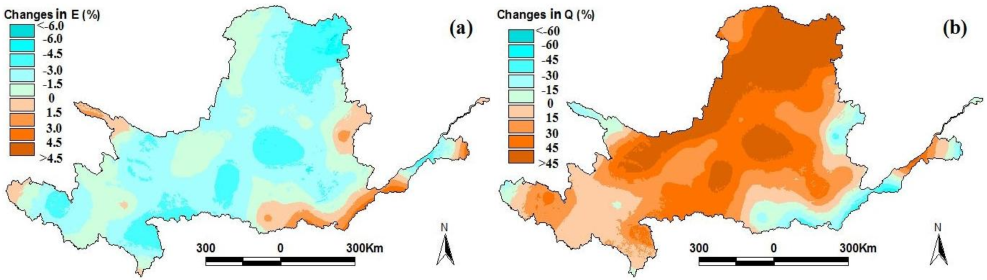

Figure 4. Modeled percent differences in mean annual total E **(a)** and Q **(b)** between static Z_e (Z_e for 1961 was fixed throughout the 1961–2010 simulation period) and dynamic Z_e (Z_e was influenced by specific water and energy conditions for each grid cell in accordance with specific climate change conditions).

HESSD
11, 11183–11202, 2014
Changes in climate or vegetation
Q. Liu et al.

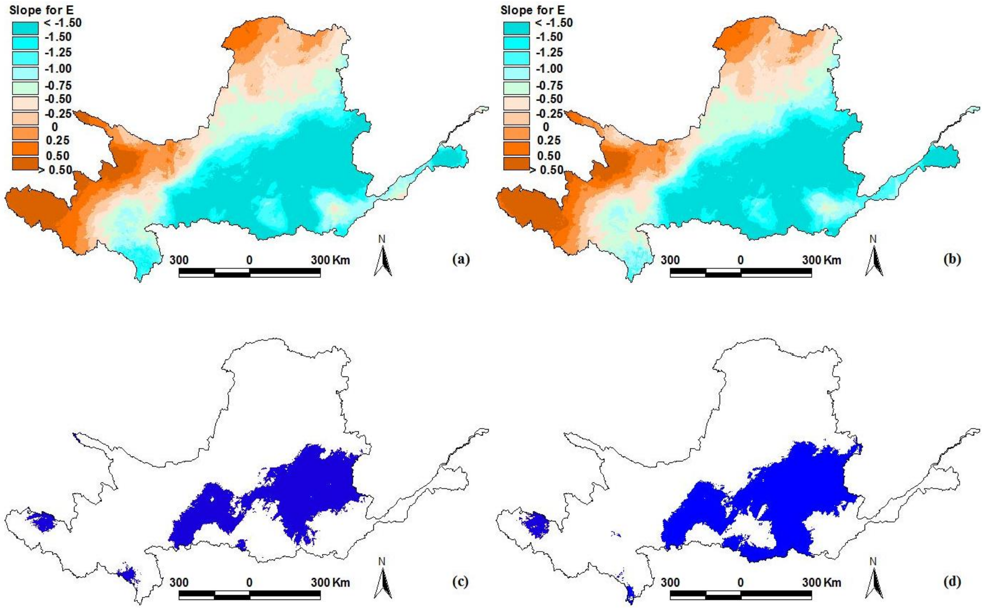

Figure 5. Temporal trends in E under dynamic Z_e **(a)** and static Z_e **(b)** scenarios, and regions exhibiting significant E slopes ($P < 0.05$) for dynamic Z_e **(c)** and static Z_e **(d)** scenarios as determined by the Mann–Kendall method.

HESSD
11, 11183–11202, 2014

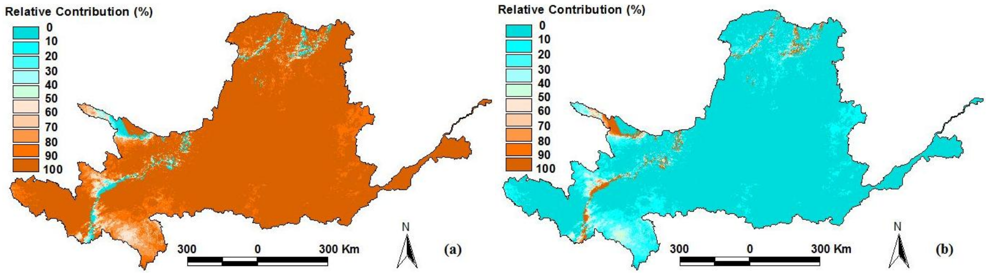

Figure 6. Relative contribution of climate **(a)** and vegetation **(b)** to changes in E.

HESSD
11, 11183–11202, 2014

Changes in climate or vegetation

Q. Liu et al.